Int. J. Heat Mass Transfer. Vol. 36, No. 9, pp. 2359–2374, 1993
Printed in Great Britain

0017–9310/93 $6.00 + 0.00

Experimental studies of forced, combined and natural convection of water in vertical nine-rod bundles with a square lattice

MOHAMED S. EL-GENK, BINGJING SU and ZHANXIONG GUO

Institute for Space Nuclear Power Studies, Department of Chemical and Nuclear Engineering, The University of New Mexico, Albuquerque, NM 87131, U.S.A.

(*Received* 1 *June* 1992 *and in final form* 9 *September* 1992)

Abstract—Experiments of upflow- and downflow-forced turbulent and laminar convection, natural convection and buoyancy-assisted combined convection of water are performed in uniformly heated, square arrayed, nine-rod bundles having P/D ratios of 1.25, 1.38 and 1.5. In the experiments, Re varies from 250 to 3×10^4, Pr from 3 to 9, Ra_q from 5×10^5 to 3×10^8 for natural convection and from 10^7 to 7×10^8 for combined convection, and Ri from 0.03 to 300. The heat transfer data are correlated in the respective convective regimes, where the heated equivalent diameter is used as the characteristic length in all dimensionless quantities and water properties are evaluated at the mean bulk temperature. The forced convection data fall into two distinct regimes: forced turbulent and forced laminar; the Reynolds number at the transition between these regimes is a linear function of P/D. In the forced convection experiments the flow is hydrodynamically developing, but thermally fully developed. The natural convection data are correlated to within $\pm 10\%$ in terms of Ra_q and the combined convection data are correlated to within $\pm 15\%$ by superimposing the Nusselt numbers, raised to the fourth power, of forced laminar and natural convection. For all P/D values, the transition from forced laminar to combined convection occurs at $Ri = 2.0$. A comparison with triangularly arrayed rod bundles shows that for the same flow area per rod, the rod arrangement negligibly affects Nu in both forced and natural convection regimes.

1. INTRODUCTION

FORCED, combined and natural convection of water in vertical, multi-rod bundles are of particular importance to many engineering applications. Examples of such applications include the design and operation of heat exchangers, steam generators, and operation and safety of nuclear reactors for both research and commercial power generation. For instance, advanced light water nuclear reactor designs currently being developed rely on natural and combined convection for passive removal of the decay heat from the reactor core after shutdown. Therefore, it is important to develop reliable heat transfer correlations for natural and combined convection regimes in vertical rod bundles. Numerous studies of heat transfer in rod bundles have been conducted, but until recently [1–4], little experimental data and heat transfer correlations had been reported for forced laminar, natural, and combined convection of water. As shown in Figs. 1(a) and (b), except for the work of El-Genk and co-workers [1–4], most heat transfer data for forced convection of water in rod bundles, with either a square or a triangular lattice, had been limited to upflow conditions at $Re > 6000$ [5–9]. No heat transfer correlation had been developed for forced laminar, natural, or combined convection in rod bundles with open flow conditions and only a few data had been reported at low Reynolds numbers ($Re < 6000$) with either isothermal or uniformly heated wall [10–14].

Although extensive theoretical studies of fully developed forced laminar and combined flows in multi-rod bundles have been performed; to the best of our knowledge results had never been confirmed by experimental data [15–22]. Because the effects of inter-subchannel cross-flow and buoyancy-induced flow mixing are difficult to model, the use of theoretical results of heat transfer in bundles is restricted to steady and fully developed flow conditions, which are of limited practical application.

El-Genk and co-workers have collected and correlated heat transfer data for forced turbulent, forced laminar, combined and natural convection of water in uniformly heated, triangularly arrayed, seven-rod bundles with P/D ratios of 1.25, 1.38 and 1.5 [1–3]. Their forced convection data fell into two distinct regimes: forced turbulent and forced laminar convection; the Reynolds number at the transition between these two regimes, Re_T, was a linear function of P/D ($Re_T = 10^4 \times (1.319\ P/D - 1.432)$. When the equivalent hydraulic diameter was used as the characteristic length in Nu and Re and the water properties were evaluated at the bulk temperature the forced turbulent convection data were within less than $\pm 10\%$ of the previously reported correlation by Weisman [23]. The natural convection data for both P/D of 1.38 and 1.5 were correlated in terms of Ra_q as $Nu_{N,L} = 0.272\ Ra_q^{0.25}$ and the combined convective data were correlated by superimposing Nusselt number correlations for forced laminar

NOMENCLATURE

A	flow area per rod [m^2]
C_p	specific heat [kJ kg^{-1} K^{-1}]
D	rod diameter [m]
D_e	equivalent hydraulic diameter, $D[(4/\pi)(P/D)^2-1]/[(4/\pi)(P/D)+1]$ [m]
D_{eh}	heated equivalent diameter, $D[(4/\pi)(P/D)^2-1]$ [m]
g	acceleration of gravity [m s^{-2}]
Gr_q	Grashof number based on heat flux, $g\beta q D_{eh}^4/kv^2$
k	thermal conductivity of water [kW m^{-1} K^{-1}]
L	length of the heated section [m]
l_{en}	entry length in rod bundles [m]
l_h	hydrodynamic entry length [m]
Nu	Nusselt number, $qD_{eh}/k(T_w-T_b)$
Nu_z	local Nusselt number
$Nu_{C.L}$	Nusselt number for combined laminar convection
$Nu_{F.L}$	Nusselt number for forced laminar convection
$Nu_{F.T}$	Nusselt number for forced turbulent convection
$Nu_{N.L}$	Nusselt number for natural laminar convection
P	pitch between adjacent rods [m]
p	power dissipated in test section [kW]
Pr	Prandtl number, $C_p\mu/k$
P/D	pitch-to-diameter ratio
q	surface heat flux, $p/9\pi DL$ [kW m^{-2}]
Ra_q	Rayleigh number, $Gr_q\,Pr$
Re	Reynolds number based on heated equivalent diameter, $\rho v D_{eh}/\mu$
Re_{D_e}	Reynolds number based on hydraulic equivalent diameter, $\rho v D_e/\mu$
Re_T	Reynolds number at the transition between forced turbulent and laminar flow regimes
Ri	Richardson number, Gr_q/Re^2
T_b	bulk temperature of water based on heat balance [K]
T_w	average wall temperature of the heated section [K]
v	average flow velocity [m s^{-1}]
z	axial distance from the entrance of the heated section [m].

Greek symbols

β	volumetric thermal expansion coefficient [K^{-1}]
ε	porosity of rod bundles, $((1-(\pi/4))(D/P))^2$
μ	dynamic viscosity [kg m^{-1} s^{-1}]
ν	kinematic viscosity [m^2 s^{-1}]
ρ	density [kg m^{-3}].

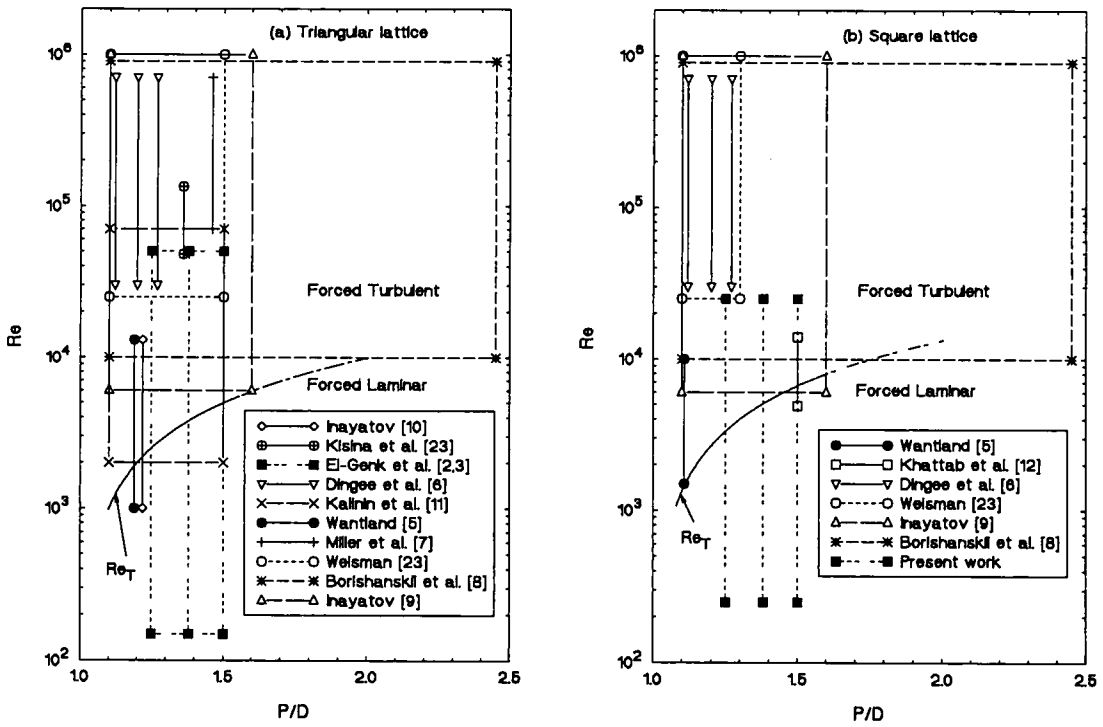

FIG. 1. Reported work on forced convection of water in vertical, multi-rod bundles: (a) triangular lattice; (b) square lattice.

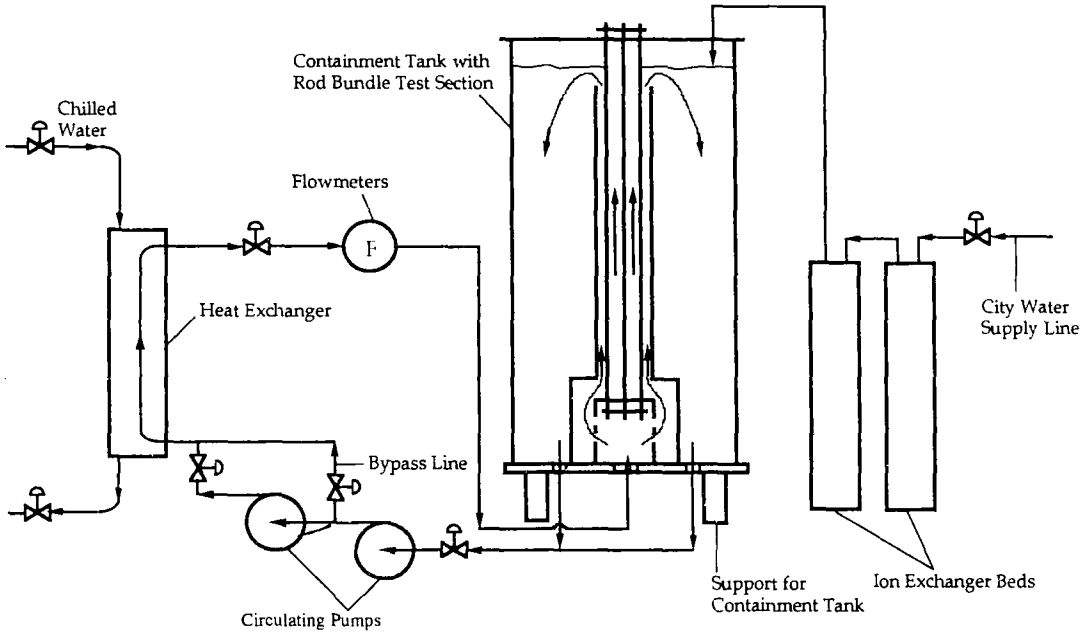

FIG. 2. A schematic of the setup for forced upflow experiments.

and natural convection using the approach first suggested by Churchill [24] as

$$Nu_{C.L} = [Nu''^{n}_{F.L} \pm Nu''^{n}_{N.L}]^{1/n}$$

the positive and negative signs indicate buoyancy-assisted and buoyancy-opposed flow condition, respectively. The value of the exponent n was 3 and 2 for buoyancy-assisted and buoyancy-opposed combined convection, respectively [3]. The transition from forced laminar to combined convection occurred at $Ri = 1.0$ for upflow and at $Ri = 0.1$ for downflow [1–3].

This paper extends the data base of El-Genk and co-workers [1–3] to square arrayed, vertical rod bundles (see Fig. 1(b)). Heat transfer experiments of upflow and downflow forced turbulent and laminar convection, natural and buoyancy-assisted combined convection of water were performed in uniformly heated, nine-rod bundles having P/D values of 1.25, 1.38 and 1.5. To quantify the effect of rod arrangement on heat transfer, the data and correlations developed in the respective flow regimes were compared with those reported previously by El-Genk *et al.* [1–3] for triangularly arrayed rod bundles.

2. EXPERIMENTAL SETUP

Figure 2 shows the experimental setup for the forced upflow experiments and Fig. 3 presents cross-sectional views of the test section assembly and rod bundle. As shown in Fig. 3, the test section consists of nine rods enclosed in a square Plexiglas shroud. The spacing between the rods was maintained using Plexiglas spacers above and below the heated section. Each test rod consists of three sections: a heated section at the middle and two unheated sections at the top and bottom ends. The heated section, a 90.4 cm long stainless steel tube (1.27 cm o.d. and 0.089 cm thick), was silver soldered at the top and bottom to the unheated sections. The unheated sections were made of 51.3 cm long brass rods, except for the central instrumented rod where the top unheated section was made of a brass tube with the same diameter and wall thickness as the heated section. The unheated sections serve as entry lengths for the hydrodynamic development of the flow before entering the heated section and for minimizing the exit effect on the heat transfer in the heated section.

The shrouded rod bundle (see Fig. 3) was supported at the bottom by a structure consisting of two concentric Plexiglas cylinders. Each cylinder has eight longitudinal openings (each is 17 cm long and 2.54 cm wide), placed 45 deg apart, in order to allow flow circulation through the test section during both forced convection and natural convection experiments. The openings in the outer cylinder were closed during the forced convection experiments, but were left open during the natural convection experiments. During the natural circulation experiments no flow was allowed to circulate through the external loop. The water entering the test bundle from the containment tank through the openings in the bottom structure (see Fig. 3) rises in the heated section under the effect of buoyancy, then returns to the containment tank. The containment tank is a Plexiglas cylinder, 61 cm o.d. and 244 cm high. As shown in Fig. 2, in the forced convection experiments the flow was circulated through the test section and the external loop by two centrifugal pumps, which provide a maximum flow rate of 1.6 kg s^{-1}. A heat exchanger with 500 kW thermal rejection capability was installed in the loop

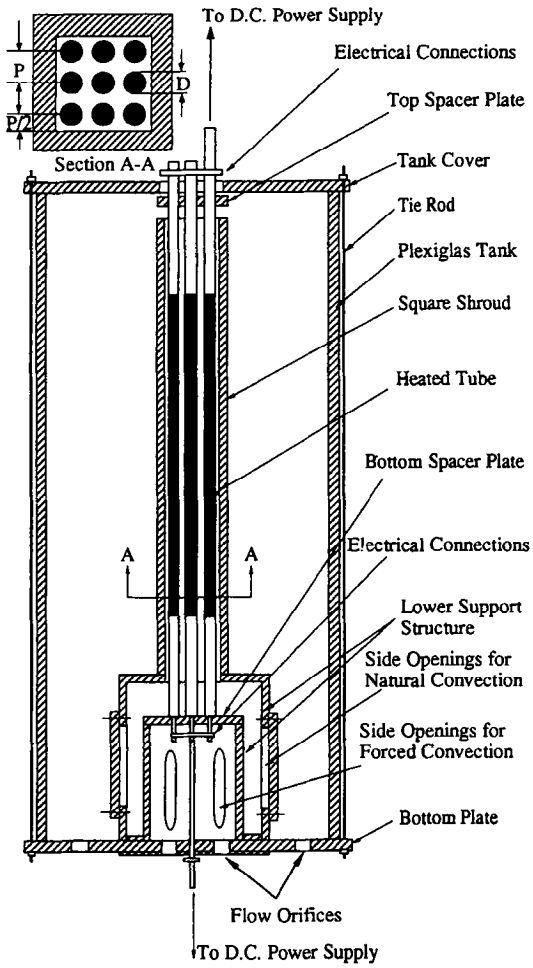

FIG. 3. Longitudinal and cross-sectional views of the containment tank and the test rod bundle.

to cool the water and help maintain a desired water temperature at the inlet of the test section. To minimize the deposition of minerals on the surface of the heated rods, the water was demineralized using ion exchanger beds and its resistivity was kept at about 14–18 MΩ cm.

3. EXPERIMENTAL MEASUREMENTS AND PROCEDURES

The power dissipated in the heated section of the rods was determined from measurements of the electric current and voltage in the test bundle, after subtracting the energy dissipated in the top and bottom brass sections, which amounted to about 3.7% of the electric power input [25]. In the forced convection experiments, the electric power dissipated in the heated section was also calibrated using the heat balance method, the measured mass flow rate and both the water inlet and exit temperatures. The agreement between the electric power dissipated and that calculated by the heat balance method was within $\pm 2\%$. In the natural convection experiments, since direct measurement of the flow rate was not possible, the energy dissipation in the heated section was determined from the electric power measurements. The maximum error in electric power measurements was less than $\pm 3\%$.

The water flow rate in the forced convection experiments was measured using a total of three flow meters covering a range from 0.013 to 1.6 kg s^{-1}; two turbine flow meters were connected in parallel for flow rates from 0.13 to 1.6 kg s^{-1}, and a rotameter for flow rates below 0.13 kg s^{-1}. Before conducting the experiments, the flow meters were calibrated and the data were used to develop calibration curves for the data analysis software; the calibration curves were within $\pm 2.5\%$ of measured values [25].

Only the central rod in the test bundles was instrumented with eight chromel–alumel (type-K) thermocouples to measure the inner surface temperatures of the heated tube wall using a specially designed Teflon probe [1–3, 26]. The inner wall temperatures were measured at eight axial locations, 4.5, 16.2, 27.8, 39.4,

51.0, 62.7, 74.3 and 85.9 cm, respectively, from the top of the heated section. These temperatures were used to determine the outer surface temperatures of the wall after taking into account the heat conduction in the wall. The difference between the inner and the outer wall surface temperatures was in the order of 0.1–1 K, depending on the operating power levels [25]. The water temperatures at the inlet and exit of the heated section were monitored using two thermocouples, placed about 5 cm above and below the heated section. The bulk water temperatures at the different axial locations in the heated section were determined from the overall heat balance using the measured flow rate, power dissipated in the heated section, and the measured inlet water temperature.

The physical properties of water in the dimensionless quantities such as Nu, Re, Pr, Gr_q, Ra_q, and Ri were evaluated at the mean bulk temperature of water in the heated section. The difference between the average outer surface temperature of the heated wall and the mean bulk temperature of water was used to determine the average value of Nu in the heated section. The values of the local Nusselt number, Nu_z, were used to verify if the flow in the forced convection experiments was thermally developed (see Results and Discussion for details). The calibration of the thermocouple in the experiments indicated a relative error of less than 0.5% in the temperature range of interest (283–363 K). The relative errors in the measured variables (electric power, temperatures, P/D ratio and flow rate) resulted in approximately $\pm 7.6\%$ uncertainty in Nu, $\pm 5.6\%$ in Re, $\pm 2.6\%$ in Pr, ± 9.5 to 13.8% in Ra_q, and ± 13.6 to 16.9% in Ri [25]. These uncertainties were calculated using the method of Kline and McClintock [27]. The main contributors to the uncertainty in Nu were the temperature and electric power measurements, the mass flow rate in Re, and the P/D in Ra_q and Ri.

In the experiments, electric power was increased from 0.5 to 13 kW in increments of about 1 kW. At each power level the flow rate was reduced from 1.6 to about 0.016 kg s^{-1} in increments of approximately 0.03 kg s^{-1} at high flow rates and 0.006 kg s^{-1} at low flow rates. The inlet water temperature was varied from 286 to 296 K. At each flow rate, after reaching steady-state, the temperatures, electric power and flow rate were recorded by a data acquisition system controlled by a personal computer. These procedures continued until a flow rate of 0.016 kg s^{-1} or a maximum wall temperature of 358 K was reached. At higher temperatures, bubbles of dissolved air were seen forming within the heated section, causing oscillation in the surface temperature measurements. The Re was varied from 250 to 3×10^4, Pr from 3 to 9, Ra_q from 5×10^5 to 3×10^8 for natural convection and from 10^7 to 7×10^8 for combined upflow and Ri from 0.03 to 300. Details of the experimental setup and conduct, calibration and measurement uncertainties, and a listing of experimental data in the various convection regimes are available elsewhere [25].

4. RESULTS AND DISCUSSION

In this section, the heat transfer data in the forced, natural and combined convection regimes in the nine-rod test bundles are presented and correlated in the respective convection regimes using the appropriate dimensionless parameters. Because the present correlations are based on the central rod temperature measurements, the heated equivalent diameter, D_{eh}, rather than the conventional hydraulic equivalent diameter, D_e, was used as the characteristic length in the dimensionless parameters such as Re, Nu, Gr_q, Ra_q and Ri. The water physical properties were evaluated at the mean bulk temperature, except for Nu_z and the local Reynolds number where the properties were evaluated at the local bulk temperature.

4.1. *Flow conditions in forced convection experiments*

Before the heat transfer data in the forced convection regimes were correlated, the hydrodynamic and thermal conditions of the flow in the heated test section for all P/D values were examined. The hydrodynamic entry length, L_h, for the flow to be hydrodynamically fully developed was calculated by the formula suggested by White [28]: $L_h = D_e[0.04\, Re_{D_e} + 0.5]$. The ratio of L_h to the length of the unheated sections in the test bundles (51.3 cm), L_{en}, is plotted against Re/Re_T in Fig. 4, where Re_T is the Reynolds number at the transition between forced turbulent and forced laminar flow regimes. In Fig. 4, the forced turbulent convection regime occupies the space where $(Re/Re_T) \geqslant 1$, and the forced laminar convection regime occupies the space where $(Re/Re_T) \leqslant 1$. When (L_h/L_{en}) is greater than unity, the flow is hydrodynamically developing, otherwise it is hydrodynamically fully developed before entering the heated section. Results in Fig. 4 demonstrate that in the forced turbulent convection experiments the flow in the heated section was hydrodynamically developing, irrespective of P/D ratio. In the forced laminar convection experiments, the flow was hydrodynamically developing in the bundle with $P/D = 1.5$; it was mostly hydrodynamically developing at the lower P/D of 1.38 and 1.25, and hydrodynamically fully developed at low Re.

In order to determine the thermal condition of the flow in the forced convection experiments, Nu_z was plotted vs axial distance from the entrance of the heated section in Figs. 5 and 6. In the upflow experiments the flow was thermally fully developed, regardless of P/D (see Fig. 5), and in the downflow experiments the flow was thermally fully developed, except for $z/L < 0.2$ and $P/D = 1.38$ and 1.5 (see Fig. 6). As shown in Fig. 5, Nu_z was almost uniform along the heated length, with maximum variation of about 10%, which could partially be attributed to cross-flow mixing among subchannels in the bundle. In Fig. 6, Nu_z decreased with axial distance up to $z/L = 0.2$, then became almost independent of axial location. In conclusion, in the forced convection experiments for all

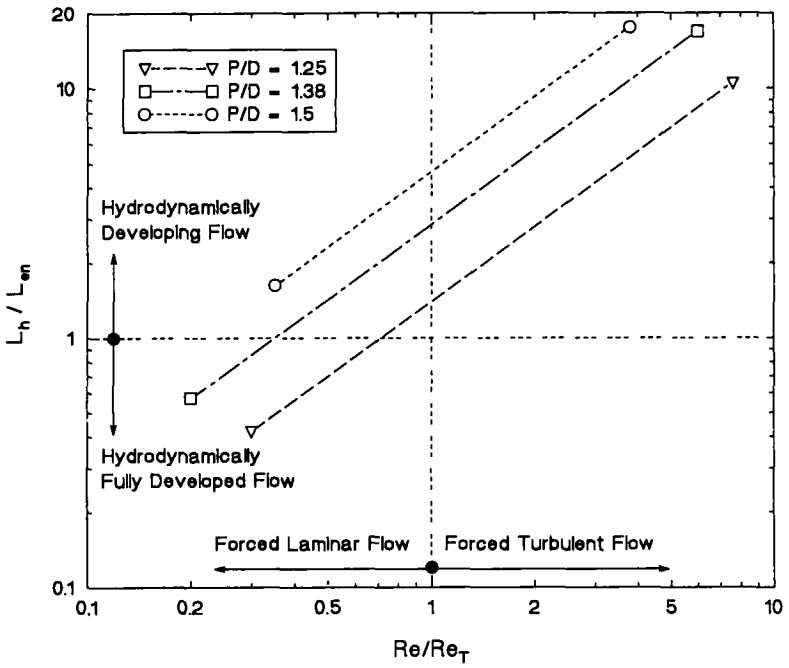

FIG. 4. Flow hydrodynamic conditions in the forced convection experiments.

P/D values the flow in the heated section was mostly hydrodynamically developing but thermally fully developed.

4.2. *Forced convection*

The heat transfer data and correlations in the forced convection regimes are presented in Figs. 7(a)–(c). These figures indicate that irrespective of the flow direction, the forced convection data can be classified into two distinct regimes: forced turbulent and forced laminar, where the Reynolds number at the transition between the two regimes, Re_T, was a linear function of P/D as

$$Re_T = 1.33 \times 10^4[(P/D) - 1]. \quad (1)$$

As shown in Fig. 8, the values of Re_T were in excellent agreement with that reported by Wantland for a square lattice [5]. For a triangular lattice, the correlation of Kim and El-Genk [1, 26] was in good agreement with the data of Inayatov [9], but higher than those reported by other investigators [5, 11]. However, the difference in Re_T between the two rod arrangements decreases as the P/D is decreased. In the forced convection regimes the data were correlated in terms of Re as:

(a) for forced laminar convection

$$Nu_{F,L} = A\, Re^B\, Pr^{0.33} \quad (2a)$$

(b) for forced turbulent convection

$$Nu_{F,T} = C\, Re^{0.8}\, Pr^{0.33} \quad (2b)$$

where

$$A = 2.97 - 1.76(P/D) \quad (3a)$$

$$B = 0.56(P/D) - 0.30 \quad (3b)$$

$$C = 0.028(P/D) - 0.006. \quad (3c)$$

As these equations indicate, the coefficient A decreased while the exponent B increased linearly with P/D (see Fig. 9(a)). In the forced turbulent convection the coefficient C in equation (2b) also increased linearly with P/D. Equations (2a) and (2b) are within $\pm 8\%$ of the experimental data [25]. Equation (2b) is also within less than 8% of Weisman's correlation [23] for squarely arrayed rod bundles (see Fig. 9(b)); Weisman's correlation was based on the fully developed turbulent upflow data of Dingee *et al.* [6] for $1.1 \leqslant P/D \leqslant 1.3$ and $Re > 25 \times 10^4$. Similar to the present work, they have used D_{eh} as the characteristic length in both Nu and Re and evaluated the water properties at the mean bulk temperature. Such good agreement establishes the soundness of the experimental setup and measurements and suggests that the Weisman correlation for square arrayed bundles could be extrapolated to higher P/D up to 1.5 and to low Re, where $Re > Re_T$ (see equation (1)).

Although the dependence of Nu for forced turbulent convection on Re was the same for both squarely and triangularly arranged rod bundles, in the forced laminar convection the dependence of Nu and Re varied not only with P/D but also with the rod arrangement. When the present results were com-

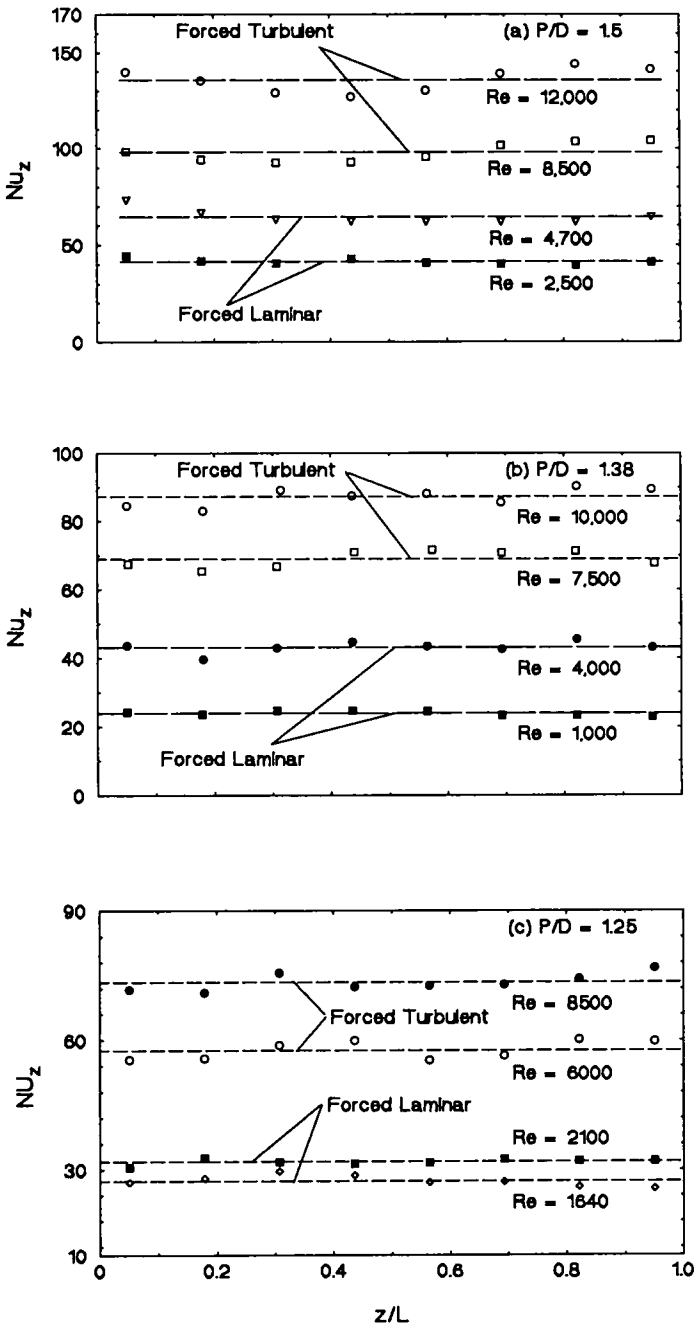

FIG. 5. Axial variation of local Nusselt number in forced upflow experiments.

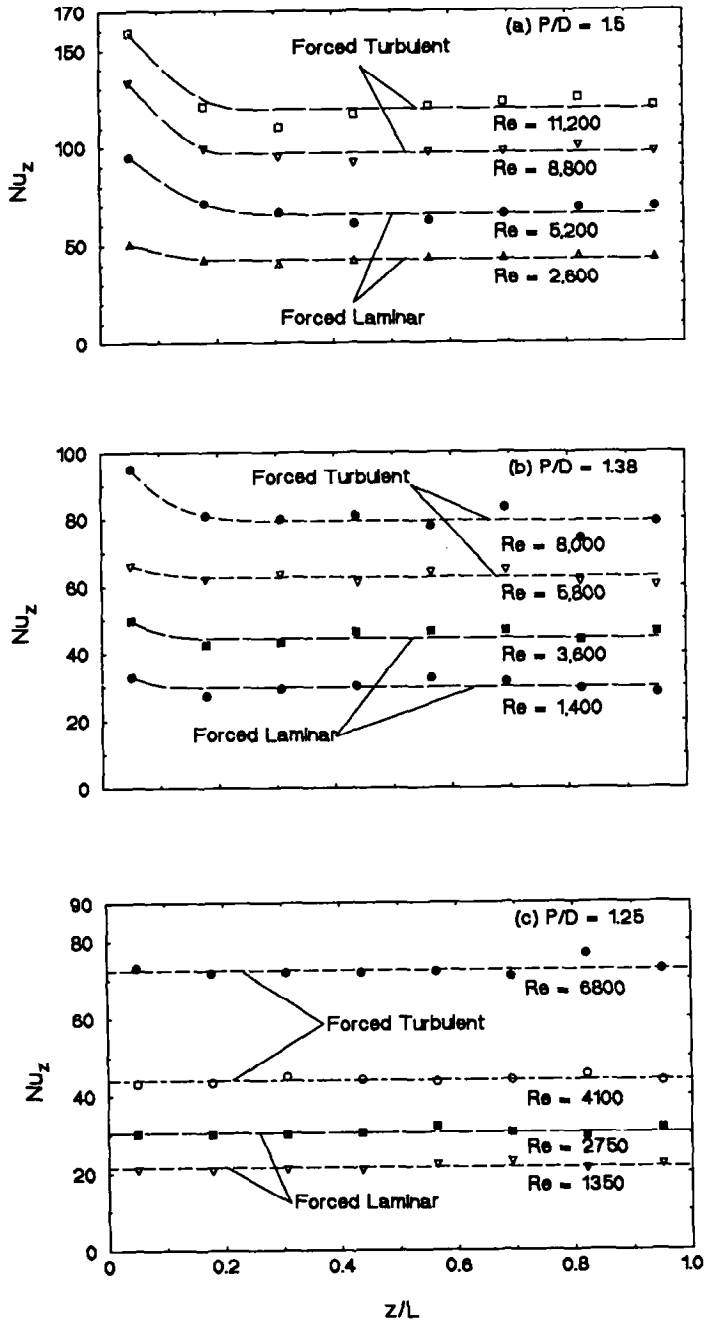

FIG. 6. Axial variation of local Nusselt number in forced downflow experiments.

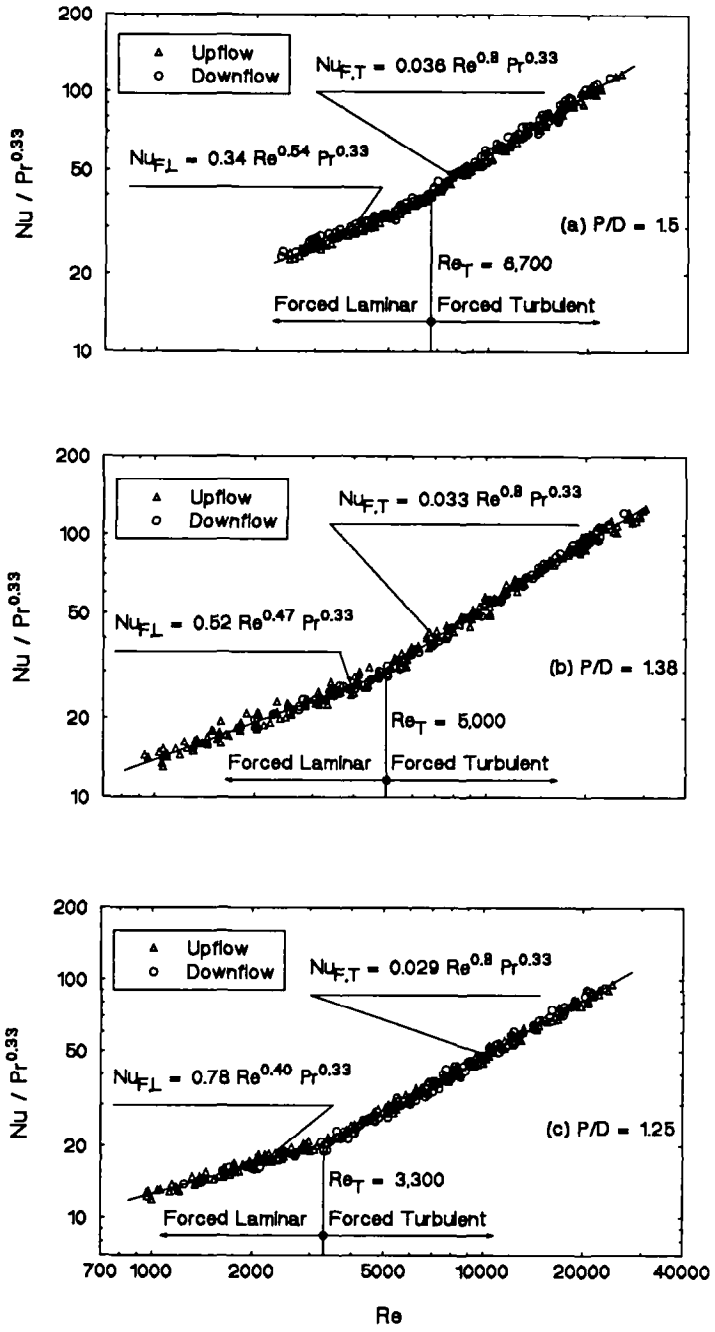

FIG. 7. Heat transfer data and correlations for forced convection regimes in a vertical, nine-rod bundle with a square lattice: (a) $P/D = 1.5$; (b) $P/D = 1.38$; (c) $P/D = 1.25$.

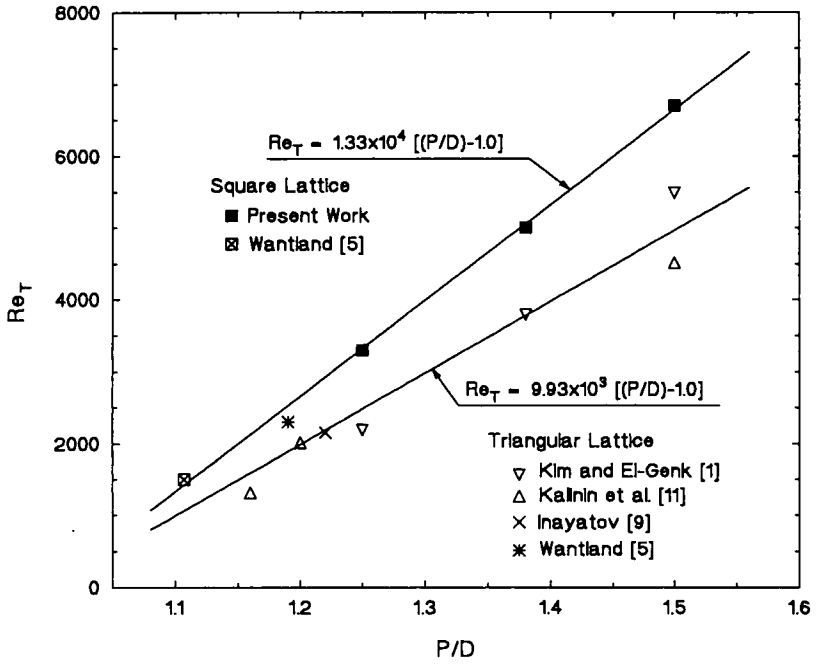

FIG. 8. Data and correlations of Re_T for triangularly and square arrayed rod bundles with different P/D ratios.

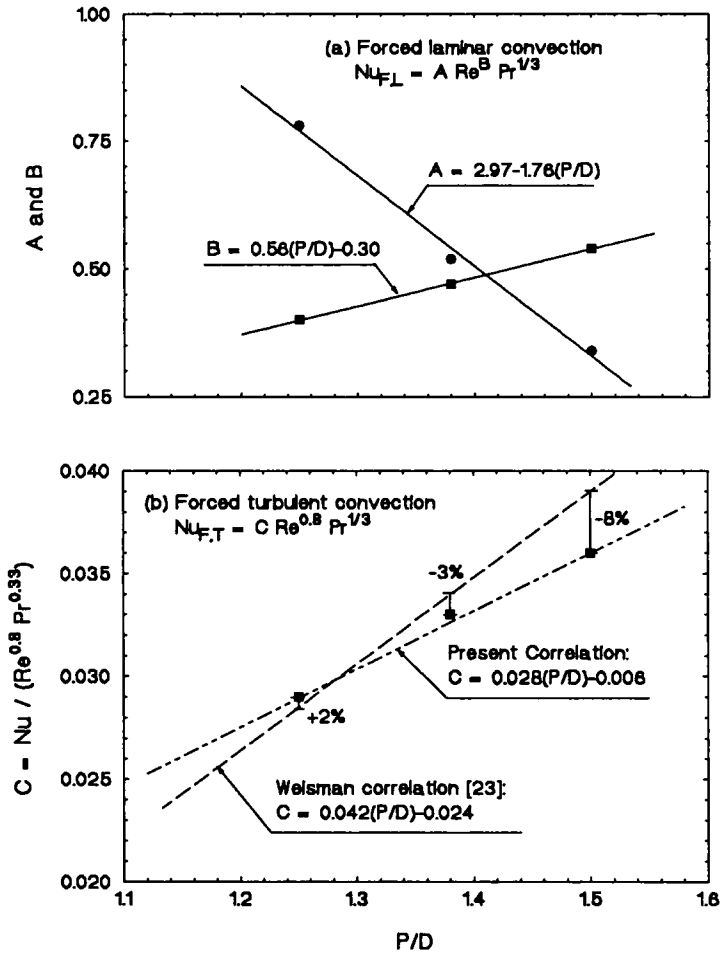

FIG. 9. Coefficients for forced convection correlations. (a) forced laminar (equation (2)); (b) forced turbulent (equation (1)).

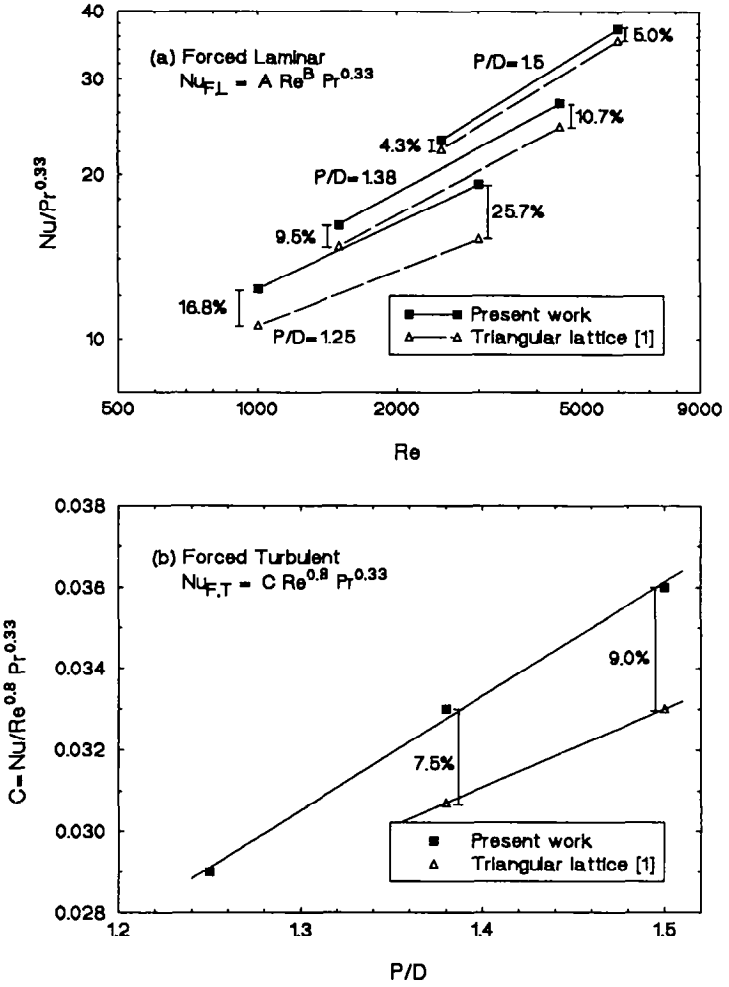

FIG. 10. Effect of rod arrangement and P/D on Nusselt number for forced convection in rod bundles.

pared with those for triangularly arrayed rod bundles, the Nusselt number for the latter was generally lower (see Figs. 10(a) and (b)). However, when the data were plotted in terms of the bundle porosity, ε, the coefficient C for forced turbulent convection was found to be independent of the rod arrangement in the bundles (see Fig. 11(b)). Similarly, in the forced laminar convection regime at a given Re, Nusselt number values increased linearly with ε, irrespective of the rod arrangements in the bundle (see Fig. 11(a)).

4.3. *Natural convection*

Natural convection experiments were performed using bundles with $P/D = 1.25$, 1.38 and 1.5. In these experiments, since buoyancy is the driving force for the flow, the heat transfer data were correlated in terms of Ra_q as

$$Nu_{N.L} = 0.178\,Ra_q^{0.27} \text{ for } P/D = 1.5 \quad (4)$$

and

$$Nu_{N.L} = 0.057\,Ra_q^{0.35} \text{ for } P/D = 1.25 \text{ and } 1.38. \quad (5)$$

In equation (4), Ra_q varied from 4×10^6 to 3×10^8, and in equation (5) it varied from 3×10^6 to 2×10^8 for $P/D = 1.38$ and from 6×10^5 to 9×10^7 for $P/D = 1.25$. As shown in Fig. 12, these correlations are in agreement with the experimental data (within $\pm10\%$) [25]. The data in Fig. 12 show that for $P/D \leqslant 1.38$ Nusselt number values were independent of P/D, which is in agreement with the work of Kim and El-Genk [1, 26] for triangularly arrayed bundles having the same rod diameter. The data also show that Nusselt number values in the bundles with a $P/D = 1.5$ were about 30% lower than those in the other two bundles with smaller P/D at $Ra_q = 3\times10^8$. However, this difference decreased as Ra_q decreased, becoming negligible at $Ra_q < 10^7$.

In Fig. 13, equations (4) and (5) were compared with that of Kim and El-Genk [1] for triangularly arrayed rod bundles and with that of Keyhani *et al.* [29] for internal circulation in a uniformly heated, square arrayed rod bundle having a $P/D = 3.08$. For consistency, the heat transfer correlation of Keyhani

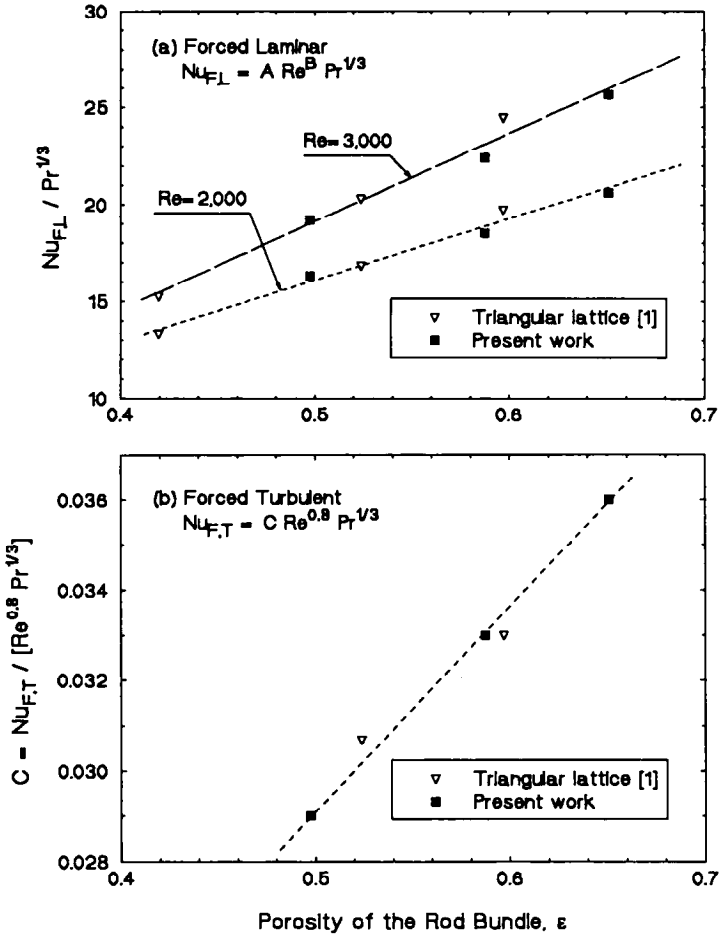

FIG. 11. Effect of rod arrangement on Nusselt number for forced convection in rod bundles as a function of the bundle porosity.

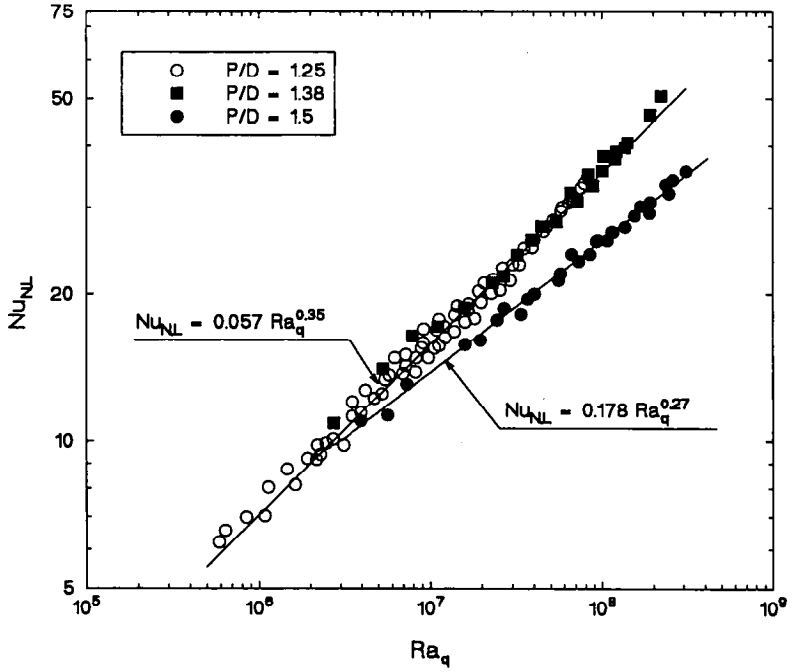

FIG. 12. Heat transfer data and correlations for natural convection in triangularly arrayed, vertical rod bundles.

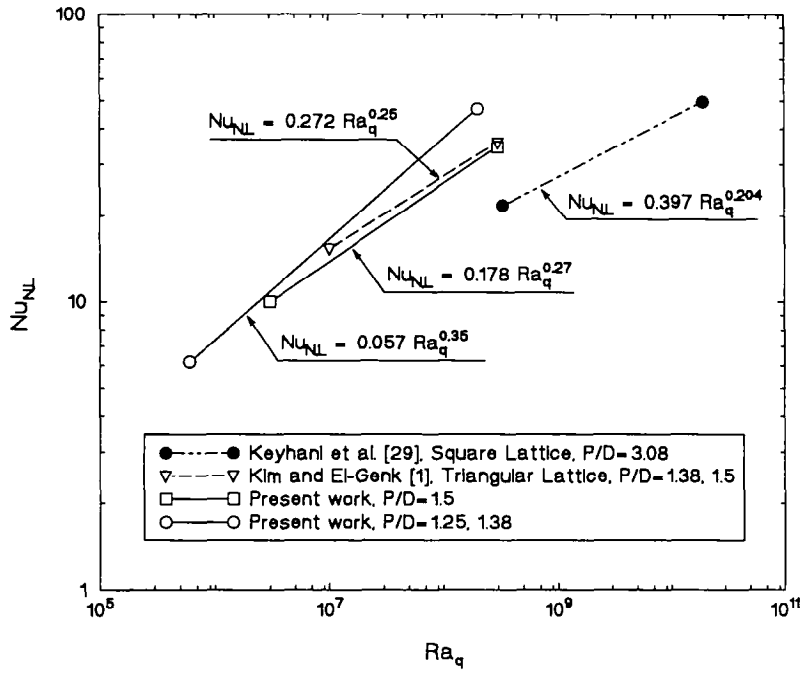

FIG. 13. Comparison of heat transfer correlations for natural convection in vertical rod bundles.

et al. [29] in Fig. 13 is represented in terms of D_{ch}, rather than the rod diameter as in the original publication. As delineated in Fig. 13, Nu for natural convection with external circulation is higher in square arrayed rod bundles than in triangularly arrayed bundles, whereas the difference in Nu decreases as Ra_q decreases. Figure 13 also shows that the correlation of Keyhani *et al.* for internal circulation is significantly lower than equations (4) and (5) and the correlations of Kim and El-Genk [1] for external circulation. This difference in Nu, which appears to decrease as Ra_q decreases, could be in part due to the larger P/D used by Keyhani *et al.*, which is consistent with the present results, and also partially due to the difference in flow conditions, internal vs external circulation.

4.4. *Combined convection*

In the combined convection regime, both inertia and buoyant forces affect heat transfer. In the upflow experiments, buoyant force accelerates the flow next to the heated wall, enhancing the heat transfer rate and causing Nu to increase with Gr_q. As indicated by Kim and El-Genk [1] and El-Genk *et al.* [2, 3], the combined convection data were better described using Ri, rather than Gr_q/Re. As shown in Figs. 14(a)–(c), the transition from forced laminar to combined convection in all three P/D values occurred at $Ri = 2.0$. This value is higher than that ($Ri = 1.0$) for triangularly arrayed rod bundles [1, 26]. Equations (2a) and either (4) or (5), depending on P/D, were used to develop a general correlation for combined convection for buoyancy-assisted flow by superimposing the two correlations as suggested by Churchill [24]. This approach has been used successfully by other investigators to correlate combined laminar flow data for isothermal and uniformly heated vertical tubes and annuli [30, 31] and by El-Genk and co-workers for uniformly heated vertical rod bundles [2, 3]. The following correlation was determined from the best fit of the buoyancy-assisted combined convection data in Figs. 14(a)–(c) as

$$Nu_{C,L} = [Nu_{F,L}^4 \pm Nu_{N,L}^4]^{0.25}. \quad (6)$$

Equation (6) fits the data for $P/D = 1.5$ to within $\pm 12\%$, and for $P/D = 1.38$ and 1.25 to within $\pm 15\%$ [25].

In Fig. 15, a heat transfer map for forced, natural and buoyancy assisted convection in square arrayed rod bundles is presented by plotting the data in terms of (Re/Re_T) on the ordinate vs Ri on the abscissa. As this figure shows, the forced turbulent convection data for all three P/D values fall in the upper half of the figure where $(Re/Re_T) \geqslant 1$, while the forced laminar convection data fall in the lower left-hand portion where $(Re/Re_T) \leqslant 1$, and $Ri \leqslant 2$. The region where $Ri \geqslant 2$, is occupied by the natural and combined convection data, for which the effect of buoyant force on heat transfer is important.

5. SUMMARY AND CONCLUSIONS

Heat transfer experiments were performed for natural and buoyancy-assisted combined convection of water in uniformly heated, square arranged, nine-rod bundles with P/D values of 1.25, 1.38 and 1.5. Experiments were also performed for hydrodynamically

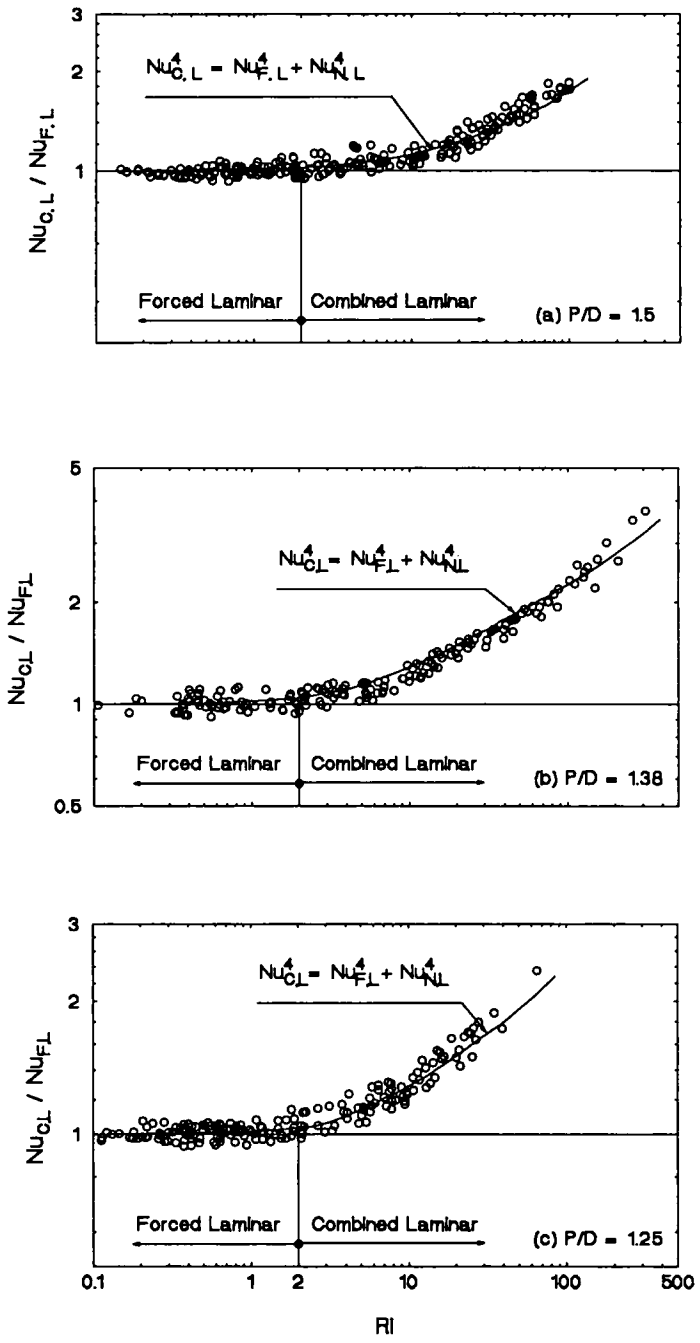

FIG. 14. Heat transfer data and correlation for buoyancy-assisted combined convection in rod bundles with a square lattice: (a) $P/D = 1.5$; (b) $P/D = 1.38$; (c) $P/D = 1.25$.

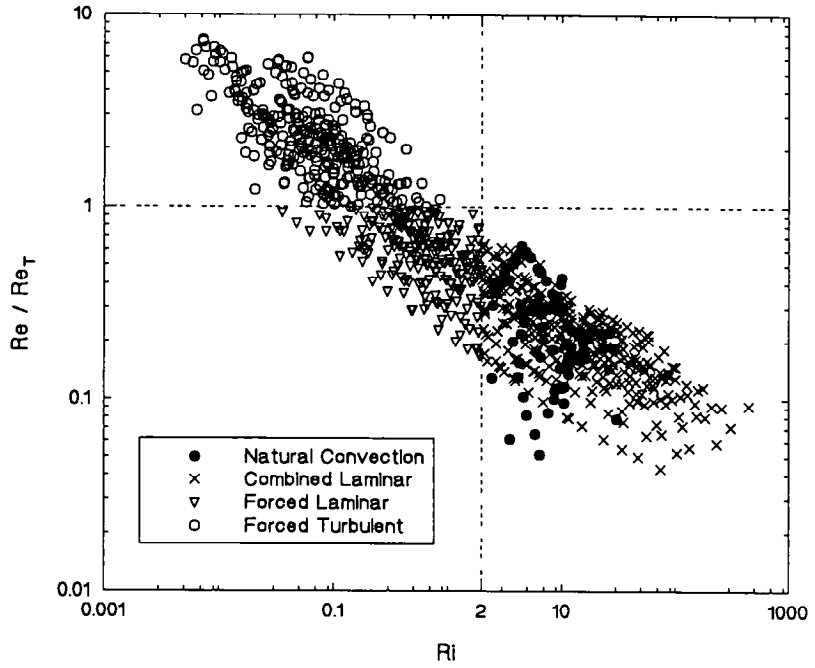

FIG. 15. Flow regime map for forced, natural and buoyancy-assisted combined convection in square arrayed, nine-rod bundles.

developing and thermally fully developed forced turbulent and laminar convections for both upflow and downflow conditions. The heat transfer data were correlated in the respective convective regimes, where the heated equivalent diameter was used as the characteristic length in all dimensionless quantities and the water properties were evaluated at the mean bulk temperature. As with triangularly arrayed rod bundles, the forced convection data fell into two distinct regimes: forced turbulent and forced laminar, where the Reynolds number at the transition between these regimes was a linear function of P/D (equation (1)). The forced turbulent convection data and correlation (equation (2b)) were within 8% of Weisman's correlation, extending its validity to low Re values ($Re > Re_T$, see equation (1)) and to higher P/D values up to 1.5. The effects of type of rod lattice on Nusselt number values for forced turbulent and forced laminar convection were found to be less than 8%. Indeed, for the same bundle porosity, ε and Re, Nu for either forced turbulent or laminar convection was independent of the rod arrangement in the bundles, and increased linearly with ε.

The natural convection data showed that for $P/D = 1.25$ and 1.38, Nu values were independent of P/D, but were higher than those for larger P/D values, with either internal or external circulation. The combined convection data were correlated to within $\pm 15\%$ by superimposing the Nusselt numbers, raised to the fourth power, of forced laminar and natural convection (equation (6)). For all P/D values, the transition from forced laminar to combined convection occurred at $Ri = 2.0$.

Acknowledgements—Research was funded by the University of New Mexico's Institute for Space Nuclear Power Studies.

REFERENCES

1. S. Kim and M. S. El-Genk, Experimental heat transfer studies for low flow of water in rod bundles, *Int. J. Heat Mass Transfer* **32**, 1321–336 (1989).
2. M. S. El-Genk, S. D. Bedrose and D. V. Rao, Forced and combined convection of water in a vertical seven-rod bundle with $P/D = 1.38$, *Int. J. Heat Mass Transfer* **33**, 1289–1297 (1990).
3. M. S. El-Genk, S. D. Bedrose and D. V. Rao, Forced and combined convection of water in rod bundles, *J. Heat Transfer Engng* **11**(4), 32–43 (1990).
4. M. S. El-Genk, B. Su and Z. Guo, Forced and combined convection of water in a 9-rod bundle with a square lattice and $P/D = 1.5$, *A.I.Ch.E. Symp. Series* **288**(88), 259–266 (1992).
5. J. L. Wantland, Compact tubular heat exchangers, *Proc. Reactor Heat Transfer Conf.* New York, TID-7529, Pt 1, Book 2, pp. 525–548 (1956).
6. D. A. Dingee, W. B. Bell, J. W. Chastain and S. L. Fawcett, *Heat transfer from parallel rods in axial flow*, Battelle Memorial Institute, Report BMI-1026 (1955).
7. P. Miller, J. J. Byrnes and D. M. Benforad, Heat transfer to water flowing parallel to a rod bundle, *A.I.Ch.E. Jl* **2**, 226–234 (1956).
8. V. M. Borishanskii, M. A. Gotovskii and E. V. Firsova, The effect of the relative spacing in heat transfer when a bundle of tubes is in the turbulent flow of a coolant ($Pr \geq 1$), *Inzh. fiz. Zh.* **19**(4), 609–616 (1970).
9. A. Ya. Inayatov, Correlation of data on heat transfer flow parallel to tube bundles at relative tube pitches of $1.1 < s/d < 1.7$, *Heat Transfer—Soviet Res.* **7**(3), 84–88 (1975).
10. A. Ya. Inayatov, Heat transfer for transitional, longitudinal flow over a tube bundle, *Inzh. fiz. Zh.* **18**(2), 353–357 (1970).
11. E. K. Kalinin, G. A. Dreitser and A. K. Kozlov, Heat

transfer in parallel-flow staggered banks of tubes with various relative spacings, *Inzh. fiz. Zh.* **16**(1), 47–53 (1969).
12. M. Kahttab, M. Mariy and M. Habib, Experimental heat transfer in tube bundle (part II), *Atomkern-energie/Kerntechnik* **45**(2), 93–97 (1984).
13. M. J. Gruszczynski and R. Viskanta, *Heat transfer to water from a vertical tube bundle under natural circulation conditions*, NUREG/CR-3167, ANL-83-7 (1983).
14. K. P. Hallinan and R. Viskanta, *Heat transfer from a rod bundle under natural circulation conditions*, NUREG/CR-4556 (1986).
15. R. W. Benodekar and A. W. Date, Numerical prediction of heat-transfer characteristics of fully developed laminar flow through a circular channel containing rod clusters, *Int. J. Heat Mass Transfer* **21**, 935–945 (1978).
16. A. Kar and R. A. Axford, Analytical study of conduction and convection heat transfer in finite tube bundles, *Nucl. Engng Des.* **107**, 253–265 (1988).
17. O. E. Dwyer and H. C. Berry, Laminar-flow heat transfer for in-line flow through unbaffled rod bundles, *Nucl. Sci. Engng* **42**, 81–88 (1970).
18. R. Mottaghian and L. Wolf, A two-dimensional analysis of laminar fluid flow in rod bundles of arbitrary arrangement, *Int. J. Heat Mass Transfer* **107**, 1121–1128 (1974).
19. K. Chen, Longitudinal laminar flow in asymmetrical finite bundles of rods, *Nucl. Engng Des.* **25**, 207–216 (1973).
20. K. Chen, On the two-dimensional analysis of fluid and heat transfer in rod bundles with arbitrary arrangement, *Nucl. Sci. Engng* **77**, 92–106 (1981).
21. K. A. Antonopoulos, Heat transfer in tube assemblies under conditions of laminar axial, transverse and inclined flow, *Int. J. Heat Fluid Flow* **6**, 193–204 (1985).
22. K. A. Antonopoulos, Heat transfer in tube banks under conditions of turbulent inclined flow, *Int. J. Heat Mass Transfer* **28**, 1645–1656 (1986).
23. J. Weisman, Heat transfer to water flowing parallel to tube bundles, *Nucl. Sci. Engng* **6**, 78–79 (1959).
24. S. W. Churchill, A comprehensive correlation equation for laminar, assisting, forced and free convection, *A.I.Ch.E. Jl* **23**(10), 10–16 (1977).
25. B. Su, *Experimental investigation on heat transfer of water in square arrayed rod bundles at low Reynolds number*, M.S. Thesis, Department of Chemical and Nuclear Engineering, University of New Mexico (1992).
26. S. Kim, *Heat transfer experiments in rod bundles at low Reynolds number*, Ph.D. Dissertation, Department of Chemical and Nuclear Engineering, University of New Mexico (1988).
27. M. Kline and F. A. McClintock, Describing uncertainties in single-sample experiments, *Mech. Engng* 3–8 (1953).
28. F. M. White, *Viscous Fluid Flow*. McGraw-Hill, New York (1974).
29. M. Keyhani, F. A. Kulacki and R. N. Christensen, Experimental investigation of free convection in a vertical rod bundle—a general correlation for Nusselt numbers, *J. Heat Transfer* **107**, 611–623 (1985).
30. M. S. El-Genk and D. V. Rao, Heat transfer experiments and correlations for low Reynolds number flows of water in vertical annuli, *Int. J. Heat Transfer Engng* **10**(2), 44–57 (1989).
31. E. Ruckenstein, Interpolating equations between two limiting cases for the heat transfer coefficient, *A.I.Ch.E. Jl* **24**, 940–941 (1978).